THE ASTROPHYSICAL JOURNAL, 611:732–738, 2004 August 20

EVIDENCE FOR EXTENDED, OBSCURED STARBURSTS IN SUBMILLIMETER GALAXIES

S. C. CHAPMAN,[1] IAN SMAIL,[2] R. WINDHORST,[3] T. MUXLOW,[4] AND R. J. IVISON[5]
Received 2004 March 5; accepted 2004 May 3

ABSTRACT

We compare high-resolution optical and radio imaging of 12 luminous submillimeter galaxies at a median $z = 2.2 \pm 0.2$ observed with the *Hubble Space Telescope* (*HST*) and the MERLIN and Very Large Array (VLA) radio interferometers at comparable spatial resolution, ~0.″3 (~2 kpc). The radio emission is used as a tracer of the likely far-IR morphology of these dusty, luminous galaxies. In ~30% of the sample the radio emission appears unresolved at this spatial scale, suggesting that the power source is compact and may be either an obscured active galactic nucleus or a compact nuclear starburst. However, in the majority of the galaxies (8/12; ~70%), we find that the radio emission is resolved by MERLIN/VLA on scales of ~1″ (~10 kpc). For these galaxies we also find that the radio morphologies are often broadly similar to their rest-frame–UV emission traced by our *HST* imaging. To assess whether the radio emission may be extended on even larger scales (≫1″) resolved out by the MERLIN+VLA synthesized images, we compare VLA B-array (5″ beam) to VLA A-array (1.″5 beam) fluxes for a sample of 50 μJy radio sources, including five submillimeter galaxies. The submillimeter galaxies have comparable fluxes at these resolutions, and we conclude that the typical radio-emitting region in these galaxies is unlikely to be much larger than ~1″ (~10 kpc). We discuss the probable mechanisms for the extended emission in these galaxies and conclude that their luminous radio and submillimeter emission arises from a large, spatially extended starburst. The median star formation rates for these galaxies are ~1700 $M_\odot$ yr^{-1} ($M > 0.1\ M_\odot$), occurring within regions with typical sizes of ~40 kpc^2 and giving a star formation density of 45 $M_\odot$ yr^{-1} kpc^{-2}. Such vigorous and extended starbursts appear to be uniquely associated with the submillimeter population. A more detailed comparison of the distribution of UV and radio emission in these systems shows that the broad similarities on large scales are not carried through to smaller scales, where there is rarely a one-to-one correspondence between the structures seen in the two wave bands. We interpret these differences as resulting from highly structured internal obscuration within the submillimeter galaxies, suggesting that their vigorous activity is producing windblown channels through their obscuring dust clouds. If correct, this underlines the difficulty of using UV morphologies to understand structural properties of this population and also may explain the surprising frequency of Lyα emission in the spectra of these very dusty galaxies.

Subject headings: cosmology: observations — galaxies: evolution — galaxies: formation — galaxies: high-redshift — galaxies: starburst — radio continuum: galaxies

1. INTRODUCTION

Since their discovery, luminous submillimeter galaxies (SMGs) have been proposed as candidates for the progenitors of the most massive spheroids in the local universe (Smail et al. 1997; Hughes et al. 1998; Lilly et al. 1999; Blain et al. 2002). Recent measurements of the redshift distribution, space densities, and clustering of this population provide strong support for this proposed relationship (Chapman et al. 2003a, 2004; Blain et al. 2004). These galaxies have large bolometric luminosities, ~10^{12}–10^{13} $L_\odot$, characteristic of ultraluminous infrared galaxies (ULIRGs; Sanders & Mirabel 1996). If their intense rest-frame far-IR emission arises from dust-obscured star formation, then the estimated rates are $\gtrsim 10^3$ $M_\odot$ yr^{-1}, sufficient to form the stellar population of a massive elliptical galaxy in only a few dynamical times, given a sufficient gas reservoir.

Alternatively, a substantial fraction of the submillimeter emission in these galaxies could arise from an obscured active galactic nucleus (AGN; e.g., Almaini et al. 1999). It has proved difficult to distinguish whether AGN or starburst activity powers the dust heating and associated far-IR radiation in these luminous SMGs (Frayer et al. 1998; Alexander et al. 2002; Chapman et al. 2003a). Optical and near-IR spectroscopy or X-ray observations have frequently been used to search for the signatures of AGNs, in both local ULIRGs and those at high redshifts (Sanders & Mirabel 1996; Fabian et al. 2000; Ivison et al. 2000; Barger et al. 2001; Frayer et al. 2003; Chapman et al. 2003a; Alexander et al. 2002, 2004; A. M. Swinbank et al. 2004, in preparation). However, merely identifying the presence of an AGN within a ULIRG does not immediately mean that it must be the dominant source of far-IR radiation. Energetic arguments must be used to estimate what fraction of a ULIRG's luminosity arises from the AGN.

A much simpler test is available if the far-IR emission is resolved. The geometry of the emission from an AGN means it is not a natural source for heating dust over an extended region; hence, any extended far-IR emission is very likely to arise from star formation. Unfortunately, the coarse resolution of most far-IR and submillimeter instruments, e.g., ~15″ FWHM at 850 μm with SCUBA on the James Clerk Maxwell Telescope, means that the emission is rarely resolved except in the most local galaxies (Le Floc'h et al. 2002). There have been

[1] Division of Physics, Mathematics, and Astronomy, California Institute of Technology, MS 320-47, Pasadena, CA 91125.
[2] Institute for Computational Cosmology, University of Durham, South Road, Durham DH1 3LE, UK.
[3] Department of Physics and Astronomy, Arizona State University, Tempe, AZ 85287-1504.
[4] MERLIN/VLBI National Facility, Jodrell Bank Observatory, University of Manchester, Cheshire SK11 9DL, UK.
[5] Astronomy Technology Centre, Royal Observatory, Blackford Hill, Edinburgh EH9 3HJ, UK.

recent claims for the detection of submillimeter emission on ~100 kpc scales around some powerful, high-redshift AGNs (Ivison et al. 2000; Stevens et al. 2003, 2004); however, these are rare and extreme objects whose characteristics may have little bearing on those of typical SMGs. To disentangle the mechanisms responsible for the far-IR emission in the population of SMGs at $z \sim 2-3$ (Chapman et al. 2003a) will likely require subarcsecond resolution to map emission on kiloparsec scales, well beyond the capabilities of current far-IR/submillimeter facilities.

One way to circumvent the limited spatial resolution of far-IR/submillimeter instruments is by exploiting the tight far-IR–radio correlation observed for infrared galaxies (e.g., Helou et al. 1985; Condon 1992) and the high angular resolution capabilities of long-baseline radio interferometers, such as the Multi-Element Microwave Linked Interferometer (MERLIN) or the Very Large Array (VLA), to infer the subarcsecond distribution of far-IR emission within SMGs. One caveat of this approach is that the far-IR–radio correlation has only been demonstrated locally on relatively large scales, ~50 kpc (Yun et al. 2001), and the precise correlation may break down on the smallest scales (M. Yun 2004, private communication). Nevertheless, if a significant extended component of the continuum radio emission from the submillimeter population is seen, then this would provide strong support for the far-IR emission being similarly extended.

The deepest 1.4 GHz observations from the VLA can detect the synchrotron-emitting disks and nuclear starbursts (formed from the coalescence of radio supernovae and their remnants) of a ULIRG, such as Arp 220, out to redshifts of $z = 3-4$. Indeed, a large fraction of the bright submillimeter population at high redshifts are detected as microjansky radio sources (Smail et al. 2000; Barger et al. 2000; Chapman et al. 2001; Ivison et al. 2002), as expected given their submillimeter luminosities and the local far-IR–radio correlation (Chapman et al. 2004). The highest spatial resolution available from the VLA at 1.4 GHz is 1.″5, but by combining deep 1.4 GHz observations from MERLIN and the VLA, it is possible to produce data sets that combine both high sensitivity and high spatial resolution, ~0.″3 scales, sufficient to map microjansky radio sources and test the extent of the far-IR activity in these galaxies.

These subarcsecond radio maps of the SMG population, which indirectly trace their far-IR morphologies, can also be compared and contrasted with the rest-frame–UV structures visible in *Hubble Space Telescope* (*HST*) imaging on similar scales. Such comparisons may help to constrain the extent of obscuration in SMGs relative to other samples of high-redshift sources selected in the rest-frame UV (e.g., Adelberger & Steidel 2000).

In this paper, we present sensitive MERLIN/VLA radio and *HST* rest-frame–UV observations of SMGs at comparable, subarcsecond resolution. We discuss the sample and observations in § 2, describe our main results in § 3, and discuss our conclusions in § 4. We assume a ΛCDM cosmology with $\Omega_0 = 0.3$, $\Omega_\Lambda = 0.7$, and $H_0 = 65$ km s^{-1} Mpc^{-1}, so that 1″ corresponds to an 8.4 kpc physical size at $z = 2.2$.

2. SAMPLE AND OBSERVATIONS

Our primary observational data set is the combined MERLIN[6] and VLA radio map of a 10′×10′ region centered on the Hubble Deep Field (HDF) region, which has sufficient sensitivity and resolution to attempt a radio morphological analysis of the SMGs in this area. The SMG sample in this region comes from the parent catalog of submillimeter-detected, optically faint microjansky radio galaxies used in the spectroscopic survey of Chapman et al. (2003a, 2004). We identify 14 submillimeter-detected galaxies lying within a 7.′5 diameter field centered on R.A. = 12^{h}36^{m}48.^{s}0, decl. = +62°15′40″ (J2000.0) that have 850 μm fluxes brighter than 4 mJy and are detected at 1.4 GHz with a flux of more than 40 μJy in the VLA A-array observations of this region. This radio flux limit should ensure a useful constraint on the source morphology from the MERLIN observations.

2.1. *MERLIN Observations*

The deep MERLIN observation of the HDF region (Muxlow et al. 1999, 2004) comprise a ~430 hr integration at 1.4 GHz of a 10′×10′ field centered on the HDF and including the Hubble Flanking Fields (HFFs). These data were acquired in 1996 February and 1997 April. The MERLIN data were supplemented with 42 hr of 1.4 GHz VLA[7] A-array observations (Richards 2000) and combined and deconvolved in the sky plane because of computational limitations. We use a map with a restored 0.″3 beam that has an rms noise level of 3.3 μJy beam^{-1}. To register the radio and optical data, radio sources associated with compact galaxies have been used to align the radio map with panoramic ground-based imaging (see below). For the HDF, this matching involves 128 $I < 24$ optical sources with radio counterparts and yields an rms of 0.″3 (Capak et al. 2004).

2.2. *HST Imaging*

We next search the *HST* database[8] for deep imaging observations of SMGs that lie within the MERLIN field. As our primary goal is a comparison of the coarse morphologies of the sources in the radio and optical wave bands, the choice of camera used for the *HST* observations is less critical than it would be for a detailed morphological analysis of SMGs (Chapman et al. 2003b). Hence, we search for any observations of SMGs within the HDF MERLIN field using the STIS and ACS cameras.

After intensive study of this field, we identify *HST* imaging of 13 SMGs from our sample that lie in the MERLIN field and list these in Table 1. Four of these galaxies come from the *HST* targeted survey of 13 SMGs observed with STIS by Chapman et al. (2003b; see Table 1). In addition to these, a further nine SMGs serendipitously fall in the HDF/HFF region, which is covered by ACS imaging from the Great Observatories Origins Deep Survey (GOODS) project (Giavalisco et al. 2004).

However, in one of these 13 sources (SMM J123651.76+621221.3), the SMG is not uniquely identified and may lie behind a foreground elliptical galaxy (Dunlop et al. 2004), and an accurate comparison of the morphology using the MERLIN/VLA radio and *HST* optical observations is impossible. We exclude this object from further comparison.

[6] MERLIN, a UK National Facility, is operated by the University of Manchester at Jodrell Bank Observatory on behalf of PPARC.

[7] The National Radio Astronomy Observatory is a facility of the National Science Foundation operated under cooperative agreement by Associated Universities, Inc.

[8] The optical data are based around observations with the NASA/ESA *HST*, obtained at the Space Telescope Science Institute, which is operated by the Association of Universities for Research in Astronomy, Inc., under NASA contract NAS5-26555.

TABLE 1
PROPERTIES OF THE SUBMILLIMETER GALAXIES

Source	Redshift	B	R	S_{850} (mJy)	$S_{1.4}$ (μJy)	Morphology	
						Radio[a]	Optical
SMM J123606.9+621021	2.51	25.6	25.2	11.6 ± 3.5	74.4 ± 4.1	E	Disturbed, merger
SMM J123616.2+621514[b]	2.58	26.8	25.7	5.8 ± 1.1	53.9 ± 8.4	E	3 components
SMM J123622.7+621630[b]	2.47	25.6	25.4	7.7 ± 1.3	70.9 ± 8.7	E	Merging disks
SMM J123629.1+621046[c]	1.01	26.1	24.6	5.0 ± 1.3	81.4 ± 8.7	E	Disturbed
SMM J123655.8+621200[d]	2.74	25.4	25.3	8.0 ± 1.8	21.0 ± 6.2	E	Disturbed, merger
SMM J123707.2+621408	2.48	26.9	26.0	6.3 ± 1.3	45.3 ± 7.9	E	Blue and red pair
SMM J123712.0+621325	1.99	26.0	25.8	4.1 ± 1.3	53.9 ± 8.1	E	Disturbed with dusty component
SMM J123712.1+621212[e]	2.91	27.0	25.5	8.0 ± 1.8	21.0 ± 4.0	E	Disturbed, double source
SMM J123618.3+621551[b]	1.87	26.0	25.9	7.3 ± 1.1	150.5 ± 11.2	C	Small group
SMM J123621.3+621708[b,f]	1.99	25.1	24.9	7.8 ± 1.9	148.1 ± 11.2	C	Linear
SMM J123635.6+621424	2.01	24.2	24.2	5.5 ± 1.4	87.8 ± 8.8	C	Disturbed, face-on spiral
SMM J123646.1+621449	1.7	25.8	25.7	10.3 ± 2.2	124.3 ± 7.9	C	Disturbed (photo-z)

[a] Radio morphologies: extended (E) or compact (C).
[b] *HST* imaging from STIS, otherwise with ACS.
[c] The radio source extends over 3.″3 predominantly to the west of the galaxy. Some very low surface brightness emission is missed in the MERLIN image, which just shows three components. There is extended emission between these sources.
[d] This source was identified in Hughes et al. (1998) as HDF 850.2.
[e] Two resolved radio sources trace the two faint UV-detected sources within a 1″ region.
[f] Two radio sources are found within the SCUBA error circle; the brighter one listed in the table lacks an optical ID, and the fainter one is associated with a linear galaxy 2″ to the east (see Fig. 1).

The Cycle 10 STIS images of galaxies in our sample use the clear imaging open filter, 50CCD (central wavelength 5733 Å), and have durations of two or three orbits (5.0–7.5 ks). The reduction and analysis of these images are described in Chapman et al. (2003b). The resolution of these images is 0.″06 FWHM, and they have a typical point-source sensitivity limit of 27.4 mag (AB).

The ACS observations of the SMGs lying within the GOODS-N field were obtained from the version 1.0 Space Telescope Science Institute (STScI) release (2003 August), in the i_{775} and b_{435} bands. The reduction of these data is described by Giavalisco et al. (2004); the typical point-source sensitivity is 28 mag (AB), and the resolution is 0.″07.

We register the *HST* images to the radio coordinate frame by aligning them with the deep SuprimeCam images from Capak et al. (2004), which are tied to the radio frame. To achieve this we first smooth the *HST* images to the ground-based seeing, then match all sources at more than 5 σ (except the SMGs) and transform the coordinate grids using the IRAF task *geotran*.

The morphological characteristics of this sample have been classified by eye from the *HST* imaging in Figure 1 and are presented in Table 1. These rough morphological classes are subject to uncertain structured dust extinction (Smail et al. 1999) and may not represent the true physical morphology of the system.

2.3. *Archival Observations*

Optical photometry for our SMG sample in the B and R bands (Table 1) was measured from the Subaru SuprimeCam imaging published by Capak et al. (2004). We use a 3″ diameter aperture centered on the radio source, and the limiting magnitudes are $B < 26.9$ and $R < 26.6$ (5 σ).

Eleven of the 12 SMGs in our sample have secure spectroscopic redshifts from the Keck survey of Chapman et al. (2004, their Table 3). These enable us to measure physical sizes and luminosities for these galaxies and also calculate K-corrections between galaxies in the sample to directly compare their rest-frame properties. *UgRIK* photometry exists for the remaining source (SMM J123646.1+621449), allowing us to estimate a photometric redshift. Using the HYPERZ software (Bolzonella et al. 2000), we derive a photometric redshift of $z = 1.7 \pm 0.2$. The median redshift of the sample is $\langle z \rangle = 2.2 \pm 0.2$, representative of that measured for larger spectroscopic samples of SMGs (Chapman et al. 2003a, 2004).

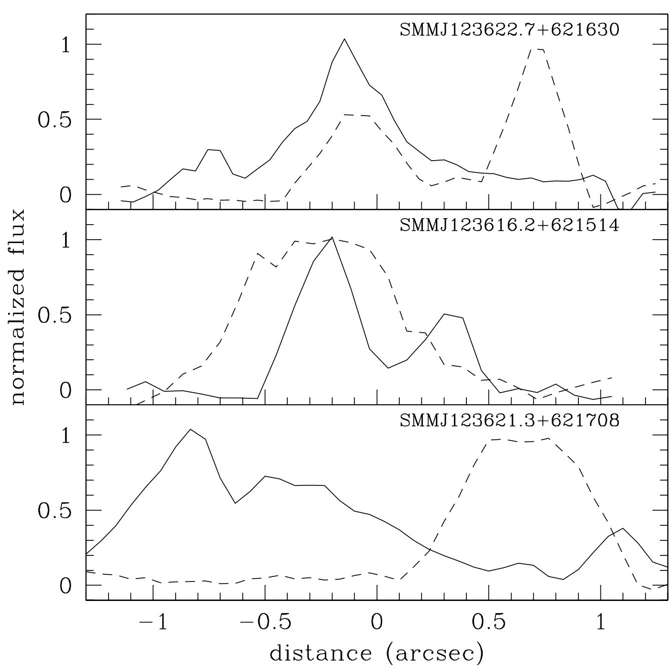

FIG. 1.—Surface brightness profiles in the radio and optical wave bands along the major axes of the radio emission in three of the resolved SMGs. The dashed line shows the radio emission from the MERLIN/VLA map and the solid line shows the equivalent distribution of the rest-frame–UV emission from the *HST* imaging. In both cases the surface brightness is averaged over a 0.″3 window orthogonal to the major axis. The bottom axis gives the angular size at the mean redshift of these three galaxies; the variation in their redshifts produces a less than 5% change in angular scale between sources.

3. ANALYSIS AND RESULTS

Using the registered radio and *HST* optical imaging, we show in Figure 1 the 1.4 GHz MERLIN/VLA contours overlaid on the *HST* images for the 12 SMGs in the joint sample. We note that at the median redshift of our sample, the *HST* imaging corresponds to rest-frame wavelengths of 1700–1800 Å. The median diameter of the radio emission from the 12 galaxies is $0\farcs83 \pm 0\farcs14$ or 7.0 ± 1.1 kpc (measured above the 3 σ contour; Fig. 1), showing that the typical source in our sample is well resolved at the resolution of our MERLIN/VLA map. The radio morphologies for these SMGs split into two broad classes: those dominated by an unresolved component, often centered on a subcomponent of the *HST* optical emission (4/12 or 33%), and extended structures on scales $\sim 0\farcs5$–1″ (8/12 or 67%). Remarkably, the extended radio morphology in these latter sources often appears to trace the same UV-bright, large-scale structures seen in the *HST* optical images (Fig. 1).

With sensitive, high-resolution imagery in the radio and optical, we can compare the radio emission (as a tracer of the dust emission) to rest-frame–UV emission on kiloparsec scales within the systems. In Figure 2 we show the radio and rest-frame–UV surface brightness profiles along the major axes of three representative resolved sources. In some cases the UV emission shows broad similarities to the radio emission. However, Figure 2 demonstrates that the UV/radio flux ratios can vary significantly over the extent of the galaxy, and the star formation rates derived from the respective wavelengths will differ accordingly. For example, in SMM J123621.3+621708 the extended rest-frame–UV emission does not trace the more compact radio emission, with the peak of the radio emission actually coinciding with a clear deficit in the UV emission. Such anticorrelations in the radio and UV are similar to those seen in many local ULIRGs (Charmandaris et al. 2002).

To test whether there is any evidence for a correlation between internal reddening and the distribution of obscured star formation traced by the radio emission, we construct ($b_{435}-i_{775}$) color maps of the 12 SMGs using the ACS imaging of the GOODS-N region. Only SMM J123712.0+621325 and SMM J123707.2+621408 show redder internal color structure that corresponds to the radio morphology. In all other cases, the radio emission does not correspond to any regions with unusually red colors in the *HST* ($b_{435}-i_{775}$) maps. SMM J123707.2+621408 and SMM J123712.0+621325 actually show bluer colors in the vicinity of the peaks in the radio emission. This suggests that the UV emission may not always probe the true site of far-IR emission; indeed, the UV-inferred bolometric luminosities in SMGs on average underpredict the true luminosities by factors $\gg 10$ (Chapman et al. 2004).

A more quantitative test of the degree of obscuration within these galaxies is gleaned through comparing the variation in the total radio/UV flux ratio measurements of each galaxy with that derived locally for the regions of intense far-IR emission pinpointed by the MERLIN/VLA morphology. The monochromatic rest-frame 2000 Å luminosities ($L_{\rm UV}$) of our SMGs are estimated from linear interpolation between the *B*- and *R*-band magnitudes (Table 1).

We estimate $L_{\rm FIR}$ using the measured radio flux (Table 1), *K*-corrected using a synchrotron slope of $\alpha = -0.75$ ($S_\nu \propto \nu^\alpha$) to rest-frame 1.4 GHz at the observed redshift and then transformed to the far-IR using the local far-IR–radio correlation from Helou et al. (1985). We take this route to estimate the far-IR emission on arcsecond scales, as our submillimeter data lack both the spatial resolution and full spectral information needed to estimate $L_{\rm FIR}$ more directly. We note that Garrett (2002) and A. Kovacs et al. (2004, in preparation) have shown that the far-IR–radio relation does not seem to change substantially out to $z \sim 1-2.5$, and so the approach we have adopted should be reliable. In this manner we predict a median total far-IR luminosity of $(3.5 \pm 1.0) \times 10^{12}\ L_\odot$ for the 12 SMGs, equivalent to star formation rates of $\sim 1700\ M_\odot\ {\rm yr}^{-1}$ for stars more massive than 0.1 $M_\odot$ based on a Salpeter initial mass function.

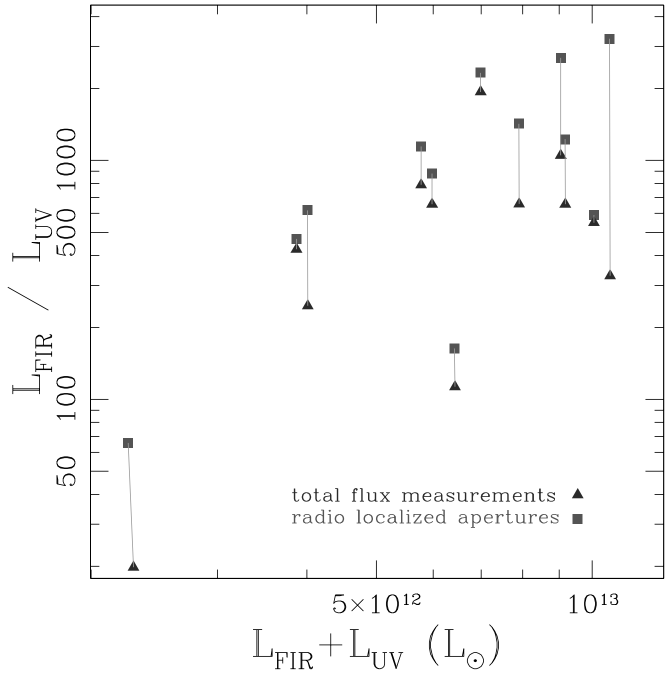

Fig. 2.—Ratio of far-IR luminosity to rest-frame–UV luminosity (2000 Å monochromatic luminosity) plotted against total luminosity (far-IR+UV) for the 12 SMGs that are detected in the MERLIN/VLA map. We show data points corresponding to the ratio derived from total flux measurements of each source using MERLIN/VLA for radio and *HST* for the rest-frame UV and based on small-aperture measurements in the UV and radio, which are based on the positions of the peak radio emission in the MERLIN/VLA map (Muxlow et al. 2004).

To investigate the variation of far-IR/UV ratios within the SMGs we first calculate the ratios for the total emission from the galaxies. We then measure the same ratio in a region encompassing the peak of the radio emission using a fixed circular aperture enclosing all radio emission above the 3 σ contour shown in Figure 1. We compare the total and locally derived $L_{\rm FIR}/L_{\rm UV}$ ratios for the 12 sources in Figure 3. We see that when the regions pinpointed as the sites of strong activity by the MERLIN/VLA radio morphology are considered, the obscuration levels increase by factors of 2–8 over the ratios derived for the whole galaxy. Even measured over the entire extent of the systems, the obscurations we derive are considerably higher than those seen in high-redshift, rest-frame UV–selected populations, which are typically $L_{\rm FIR}/L_{\rm UV} \sim 0.1-100$ (e.g., the Lyman break galaxies: Adelberger & Steidel 2000; or the BX/BM galaxies: Steidel et al. 2004).

3.1. *Searching for Very Extended Radio Emission*

Having discovered that the radio emission in over half the SMGs in our sample is extended on 1″ scales, we now wish to test whether this emission extends to even larger scales, $\gtrsim 5''$ or $\sim$50 kpc. We can constrain the fraction of radio flux arising

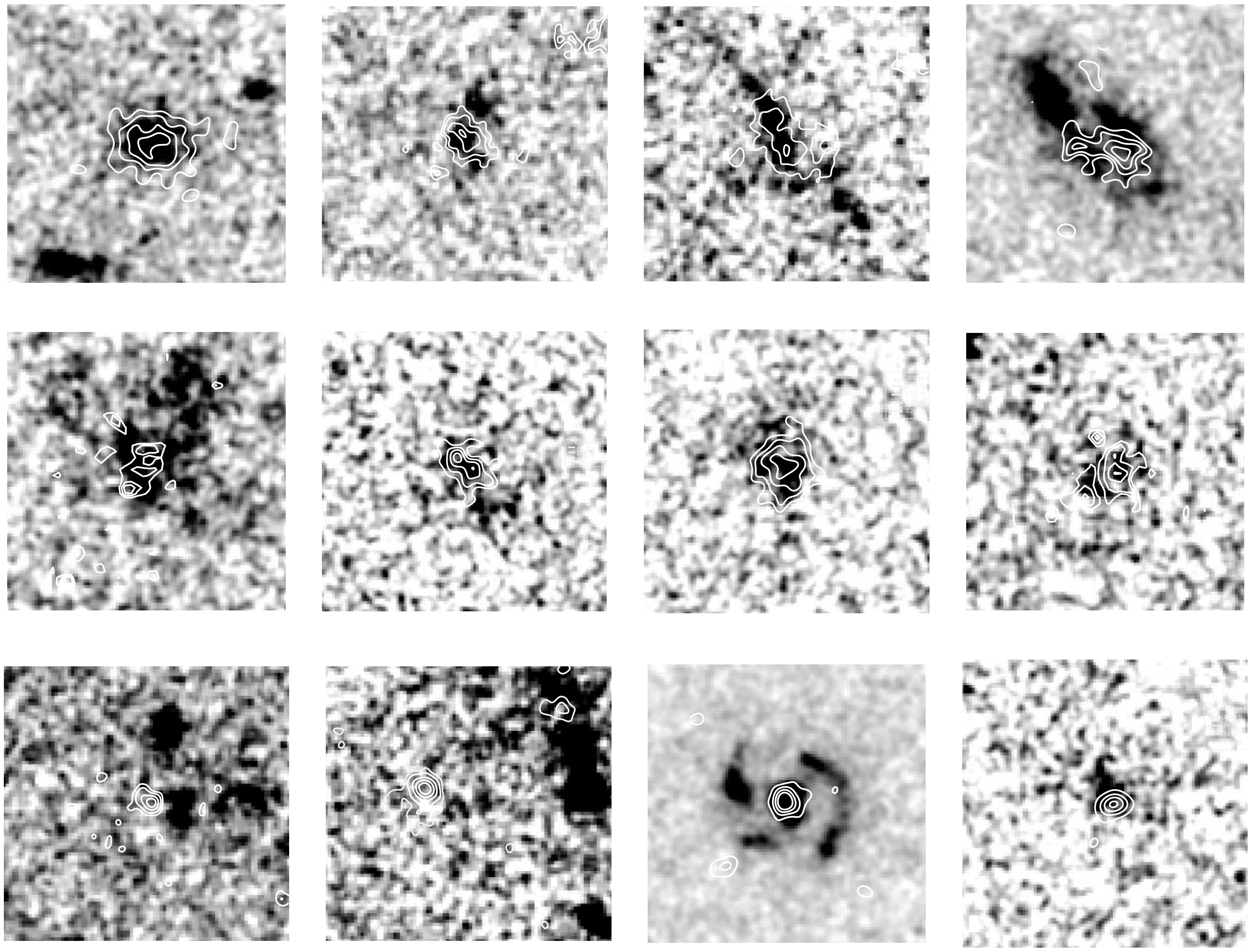

FIG. 3.—Comparison of MERLIN/VLA radio data (0.″2–0.″3 synthesized beam size, shown as contours) for 12 of our SMGs with the *HST* STIS clear imaging filter 50CCD and ACS $b_{435} + i_{775}$ imaging (as noted in Table 1). The *HST* images have been smoothed with a Gaussian of FWHM 0.″2 to match the effective resolution of the radio map. The first two rows show sources where the radio is clearly extended along a portion of the rest-frame–UV imaging, whereas the final four panels on the bottom row reveal point sources in the radio, likely associated with a single UV component. Radio contour levels begin at 3 σ and increase in linear steps scaled to the peak of the radio emission. Each panel is 3″ on a side, and they are ordered from top left as in the same sense as Table 1.

on $\gtrsim$1.″5 scales by a simple comparison of the 1.4 GHz fluxes of SMGs in maps from the VLA in its B-array (5″ synthesized beam) and A-array (1.″5 beam) configurations. The higher resolution A-array observations may resolve out a portion of the total emitted flux density of any source that has significant extended structure on scales larger than the 1.″5 VLA A-array beam. As no B-array coverage is available for the HDF-N, we have assembled VLA B-array and A-array fluxes for a sample of 50 μJy radio sources, including five SMGs, from the SSA 22 survey field (see Chapman et al. 2004).

We calculate the median and bootstrap errors on the flux ratios for the radio sources from the data taken at the two resolutions. We start by confirming that sources show either similar or higher fluxes in the B-array map compared to the A-array data, as expected considering the median radio angular sizes of microjansky sources (Windhorst et al. 1993). We find a median ratio of $\langle S_B/S_A \rangle = 1.45 \pm 0.27$, and the ratios for 30% of the sample agree within 2 σ, suggesting there is no calibration offset between the fluxes from the two maps. For the five submillimeter-detected sources we obtain a median flux ratio of $\langle S_B/S_A \rangle = 1.22 \pm 0.12$, compared to 1.22 ± 0.11 for an *R*-band matched sample of eight radio sources undetected or unobserved in the submillimeter wave band. This suggests that the submillimeter-luminous section of the microjansky radio population is no more extended than the general population after we have removed low-redshift galaxies (with bright apparent magnitudes). Moreover, we see that there is only weak evidence that the radio emission in the SMGs is extended on $\gg$10 kpc scales.

4. DISCUSSION AND CONCLUSIONS

The far-IR emission from local ULIRGs generally arises from the nuclear regions of the systems, while the UV light is more extended, although it contributes a negligible fraction of the bolometric emission (Goldader et al. 2002; Surace & Sanders 2000). We have been able to trace the distribution of these two components in similarly luminous galaxies at high redshifts through the combination of subarcsecond imagery in the radio and rest-frame UV from our MERLIN/VLA and *HST* observations. These maps allowed us to investigate the relative distribution of obscured and unobscured star formation on kiloparsec scales within luminous submillimeter galaxies at $z \sim 2.2$, when the universe was only a fifth of its current age.

As expected, the UV morphologies of this sample are similar to the (overlapping) sample of SMGs imaged with *HST* STIS and analyzed by Chapman et al. (2003b), as well as to the ACS imaging in Smail et al. (2004). The sample galaxies exhibit irregular and frequently highly complex morphologies in their rest-frame ∼2000 Å emission compared to optically selected galaxies at similar redshifts and have scale lengths far in excess of comparably luminous local galaxies.

Turning to the radio morphologies, we find that in ∼70% (8/12), the MERLIN/VLA radio images exhibit resolved radio emission on ∼0.″5–1″ scales (∼10 kpc) that mirrors the general form of the rest-frame–UV morphology seen by *HST*. We interpret this as strong support for the radio emission tracing spatially extended, massive star formation within these galaxies. This situation is very unlike local ULIRGs, where the high surface brightness far-IR/radio emission is restricted to a compact nuclear region with an extent of less than ∼1 kpc (Charmandaris et al. 2002). A more detailed analysis of the distribution of UV and radio emission within these galaxies (Figs. 2 and 3) shows that the correspondence is rarely one-to-one, with variations of the UV/radio flux ratio by factors of a few on kiloparsec scales within galaxies. It is likely that comparisons using even higher resolution data would show even stronger variations, as are seen in local ULIRGs (e.g., Bushouse et al. 2002) but are diluted at the current resolution. Similarly, there is only weak evidence for correlations between the rest-frame–UV colors and the positions of the radio-emitting regions within these galaxies. Here, longer wavelength near-IR observations with *HST* NICMOS, or from the ground, may reveal variations in the UV spectral slope that would show a better correlation of reddening with radio intensity (Smail et al. 2004).

In the remaining ∼30% (4/12) of SMGs, the radio emission is much more compact and is essentially unresolved, suggesting it arises in a region with a scale size of the order of ∼1 kpc or less (Fig. 1). In two of these cases, the compact radio emission is centered on a bright UV source (in one case clearly the nucleus of a face-on spiral galaxy, which is a strong X-ray source and is also the only one of the sources in our sample that shows AGN signatures in its UV spectrum), while in the other two systems the compact radio component is spatially offset by several kiloparsecs from the UV source. These configurations reflect compact, nuclear starbursts and/or a dominant contribution from an AGN to the radio emission. In half of these cases, the AGN/nuclear starburst is also strongly obscured at rest-frame wavelengths of ∼2000 Å.

Stevens et al. (2003, 2004) have recently presented evidence for submillimeter emission resolved on ∼100 kpc scales (including apparent filaments) in the rare and extreme environments around powerful radio galaxies and absorbed QSOs at $z \sim 2-4$. Our results demonstrate that in many cases (∼70%) the far-IR emission (as seen in our MERLIN/VLA radio maps) of the general SMG population is extended on scales of ∼10 kpc. However, the interferometric measurements are not suited to measuring larger scale, diffuse emission. Our VLA B-array versus A-array comparison (§ 3.1), however, suggests that the typical field SMG does not have submillimeter emission (as traced by the radio) extending on scales much larger than 1″ (10 kpc).

Our high-resolution radio and optical imaging allows us to address the relative obscuration of the galaxies. Adelberger & Steidel (2000) have suggested that high-luminosity galaxies at high redshift have much stronger obscuration than lower luminosity galaxies, as measured by the ratio of far-IR to rest-frame–UV luminosity. This is certainly true on large scales in the SMGs. On smaller scales within the SMGs, we have seen that the obscuration is roughly 2 times higher over the region of intense radio (and by implication far-IR) emission, compared to the average over the whole galaxy. This suggests that there is highly structured reddening within the SMGs; such anisotropic obscuration would be a natural consequence of channels being blown through the dust around the star formation regions by vigorous winds.

It is worth considering that few starburst galaxies with $L_{\rm FIR} \sim 4 \times 10^{12}\ L_\odot$ exist locally; most galaxies in our neighborhood with these luminosities have strong and obvious AGN components. However, at $z \sim 2.2$, the median redshift of the radio-selected SMGs, the most active galaxies were evidently forming stars at rates of $\sim 1700\ M_\odot\ {\rm yr}^{-1}$ in regions extending over $\sim 40\ {\rm kpc}^2$. The large physical extent of this activity contrasts markedly with the compact, nuclear starbursts typical of local ULIRGs. This suggests that some of the observational properties of the star formation activity in these galaxies (e.g., mix of dust temperatures or ease of superwind generation) may differ markedly from that seen in local "analogs." However, we also note that the star formation surface density inferred from our radio observations is $\sim 45\ M_\odot\ {\rm yr}^{-1}\ {\rm kpc}^{-2}$, comparable to the upper limit estimated for such activity in local starburst galaxies by Meurer et al. (1997). This argues that the small-scale physical mechanisms that limit the star formation process within these galaxies are similar to those operating in the most vigorous systems locally.

While evidence for massive amounts of molecular gas in SMGs has now been established (Frayer et al. 1998; Neri et al. 2003; T. Greve et al. 2004, in preparation), and X-ray luminosities are consistent with a dominant role for star formation in the energetics of SMGs (D. Alexander et al. 2004, in preparation), our discovery of spatially extended radio morphologies is perhaps the strongest piece of evidence that star formation dominates the bolometric output of the majority of the SMG population.

In summary, we have compared the rest-frame–UV and–radio morphologies on subarcsecond scales of a small sample of highly luminous, dusty galaxies for which precise redshifts are available. This analysis shows that the radio emission, which we adopt as a proxy for the far-IR emission, is resolved in the majority of galaxies, implying that dust heating (and by implication, massive star formation) is occurring on ∼10 kpc scales within these systems. Currently, this represents our only constraint on the likely submillimeter morphology of these galaxies, and it will not be further testable until the Atacama Large Millimeter Array (ALMA) comes online. The overall structure of the radio emission matches that seen in the rest-frame UV, although there are strong variations in the relative emission on kiloparsec scales, which we interpret as resulting from highly structured dust obscuration within the galaxies. This structured obscuration may reflect from anisotropic dispersal of the dust as superwinds driven by the star formation activity blows channels through the intergalactic medium. Such channels would provide the opportunity for Lyα photons to escape from these otherwise highly obscured systems, explaining the unexpected strength of this line in their spectra (Chapman et al. 2003a, 2004).

We would like to thank the anonymous referee for helpful comments that improved the clarity of the manuscript. We also thank our collaborator, Andrew Blain, for his work on the Keck SMG redshift survey. Support for proposal 9174 (S. C. C., R.W.) was provided by NASA through a grant from the Space Telescope Science Institute, which is operated by the Association of Universities for Research in Astronomy, Inc., under NASA contract NAS5-26555. I. S. acknowledges support from the Royal Society and Leverhulme Trusts.

REFERENCES

Adelberger, K., & Steidel, C. 2000, ApJ, 544, 218
Alexander, D., Vignali, C., Bauer, F. E., Brandt, W. N., Hornschemeier, A. E., Garmire, G. P., & Schneider, D. P. 2002, AJ, 123, 1149
Almaini, O., Lawrence, A., & Boyle, B. J. 1999, MNRAS, 305, L59
Barger, A., Cowie, L., Mushotzky, R., & Richards, E. 2001, AJ, 121, 662
Barger, A., Cowie, L., & Richards, E. 2000, AJ, 119, 2092
Blain, A., et al. 2002, Phys. Rep., 369, 111
———. 2004, ApJ, in press
Bolzonella, M., Miralles, J.-M., & Pelló, R. 2000, A&A, 363, 476
Bushouse, H. A., et al. 2002, ApJS, 138, 1
Capak, P., et al. 2004, AJ, 127, 180
Chapman, S. C., Blain, A., Ivison, R. J., & Smail, I. 2003a, Nature, 422, 695
Chapman, S. C., Blain, A., Smail, I., & Ivison, R. J. 2004, ApJ, submitted
Chapman, S. C., Richards, E. A., Lewis, G. F., Wilson, G., & Barger, A. J. 2001, ApJ, 551, L9
Chapman, S. C., Windhorst, R., Odewahn, S., Yan, H., & Conselice, C. 2003b, ApJ, 599, 92
Charmandaris, V., Stacey, G. J., & Gull, G. 2002, ApJ, 571, 282
Condon, J. J. 1992, ARA&A, 30, 575
Dunlop, J., et al. 2004, MNRAS, 350, 769
Fabian, A. C., et al. 2000, MNRAS, 315, L8
Frayer, D., et al. 1998, ApJ, 506, L7
———. 2003, AJ, 126, 73
Garrett, M. A. 2002, A&A, 384, L19
Giavalisco, M., et al. 2004, ApJ, 600, L93
Goldader, J., Meurer, G., Heckman, T., Seibert, M., Sanders, D., Calzetti, D., & Steidel, C. 2002, ApJ, 568, 651
Helou, G., Soifer T., Rowan-Robinson, M. 1985, ApJ, 298, L7
Hughes, D., et al. 1998, Nature, 394, 241
Ivison, R. J., et al. 2000, MNRAS, 315, 209
———. 2002, MNRAS, 337, 1
Le Floc'h, E., Charmandaris, V., Laurent, O., Mirabel, I. F., Gallais, P., Sauvage, M., Vigroux, L., & Cesarsky, C. 2002, A&A, 391, 417
Lilly, S. J., Eales, S. A., Gear, W. K. P., Hammer, F., Le Fèvre, O., Crampton, D., Bond, J. R., & Dunne, L. 1999, ApJ, 518, 641
Meurer, G. R., Heckman,T. M., Lehnert, M. D., Leitherer, C., & Lowenthal, J. 1997, AJ, 114, 54
Muxlow, T., et al. 1999, NewA Rev., 43, 623
———. 2004, MNRAS, submitted
Neri, R., et al. 2003, ApJ, 597, L113
Richards, E. 2000, ApJ, 533, 611
Sanders, D. B., & Mirabel, I. F. 1996, ARA&A, 34, 749
Smail, I., Ivison, R. J., & Blain, A. W. 1997, ApJ, 490, L5
Smail, I., Ivison, R. J., Owen, F. N., Blain, A. W., & Kneib, J.-P. 2000, ApJ, 528, 612
Smail, I., Morrison, G., Gray, M. E., Owen, F. N., Ivison, R. J., Kneib, J.-P., & Ellis, R. S. 1999, ApJ, 525, 609
Smail, I., et al. 2004, ApJ, submitted
Steidel, C., Shapley, A. E., Pettini, M., Adelberger, K. L., Erb, D. K., Reddy, N. A., & Hunt, M. P. 2004, ApJ, 604, 534
Stevens, J. A., Page, M. J., Ivison, R. J., Smail, I., & Carrera, F. J. 2004, ApJ, 604, L17
Stevens, J., et al. 2003, Nature, 425, 264
Surace, J., & Sanders, D. 2000, AJ, 120, 604
Windhorst, R., et al. 1993, ApJ, 405, 498
Yun, M., Reddy, N., & Condon, J. 2001, ApJ, 554, 803